4-9-2023

# A Critical Investigation into the Structural Behavior of Senior Design's Electric Vehicle Tube Frame Chassis Using Finite Element Analysis

Samuel Oluwademilade Aina

Jason Leroy Calkins

# A Critical Investigation into the Structural Behavior of Senior Design's Electric Vehicle Tube Frame Chassis Using Finite Element Analysis

by

**Jason Leroy Calkins and Samuel Oluwademilade Aina**

An Honors Capstone

submitted in partial fulfillment of the requirements

for the Honors Diploma

to

The Honors College

of

The University of Alabama in Huntsville

April 23, 2023

Honors Capstone Director: Dr. Nicholas Ginga, Assistant Professor - MAE

Jason Calkins, Aina 4-9-23

Student Date

4/15/2023

Director Date

4/21/2023

Department Chair Date

William Wilkerson Digitally signed by William Wilkerson
Date: 2023.04.23 14:11:40 -05'00'

Honors College Dean Date

HONORS COLLEGE
THE UNIVERSITY OF ALABAMA IN HUNTSVILLE

Honors College
Frank Franz Hall
+1 (256) 824-6450 (voice)
+1 (256) 824-7339 (fax)
honors@uah.edu

## Honors Thesis Copyright Permission

**This form must be signed by the student and submitted as a bound part of the thesis.**

In presenting this thesis in partial fulfillment of the requirements for Honors Diploma or Certificate from The University of Alabama in Huntsville, I agree that the Library of this University shall make it freely available for inspection. I further agree that permission for extensive copying for scholarly purposes may be granted by my advisor or, in his/her absence, by the Chair of the Department, Director of the Program, or the Dean of the Honors College. It is also understood that due recognition shall be given to me and to The University of Alabama in Huntsville in any scholarly use which may be made of any material in this thesis.

Jason Calkins, Samuel Aina

Student Name (printed)

Jason Calkins, Aina

Student Signature

4-9-23

Date

**Table of Contents**

**Abstract**

This capstone project explores the use of finite element analysis (FEA) to critically investigate and improve the structural properties of the chassis designs that are developed over the course of the UAH Electric Vehicle (EV) Senior Design class. Increasing the torsional stiffness and optimizing chassis weight were the main focuses of this project. The benefits and reasoning behind using torsional stiffness as a primary metric and using finite element analysis to model it were also explored. This analysis aided in improving the performance of the vehicle and allowed the chassis team to have confidence that the chassis is structurally sound and safe. By the conclusion of the project, through analysis and modification, we were able to achieve a torsional stiffness comparable with similar designs from other universities without adding significant weight. Each chassis design iteration was modeled and through these models and results we were able to improve the torsional stiffness of the chassis by 36.8%, from 1099 $\frac{N \cdot m}{degree}$ to 1503 $\frac{N \cdot m}{degree}$, by the time the chassis was released for manufacturing. Additionally, we conceptualized, designed, and manufactured a physical testing device to validate the computer models for the torsional stiffness of the chassis. This physical torsion testing jig experimentally provided a torsional stiffness value for the manufactured chassis of 1360 $\frac{N \cdot m}{degree}$. The experimentally gathered physical value differed only 10% from the expected stiffness value found through FEA, thus confirming the validity of our design.

# Introduction

## Electric Vehicle Senior Design

SAE International organizes Formula SAE (FSAE), a student design competition. The competition was launched by the SAE student branch at the University of Texas at Austin in 1980 after a previous racing contest failed. The objective of Formula SAE is for a student design team to build a small Formula-style racecar for a fictional manufacturing company. This racecar is then evaluated for its potential as a production item. Each student team is tasked with designing, building, and testing a prototype based on a series of rules, with the purpose of ensuring on-track safety and promoting clever problem solving. The cars are then tested in a series of events designed to challenge the vehicle's maneuverability, structure, endurance, and speed ("FSAE History").

Initially a competition for internal combustion engine vehicles, FSAE added the battery electric class to the competition in 2013. In Fall 2020, the University of Alabama in Huntsville (UAH) started a senior design class where the students designed an FSAE electric vehicle (FSAE-EV). Presently during the 2022-2023 term, under Dr. Nicholas Ginga, the third iteration of this project has been building on the work of previous years' teams and was tasked with the design and manufacturing of a fully functional rolling prototype capable of housing and supporting all other systems within the vehicle. The main systems for the 2022-2023 iteration consisted of the chassis, suspension, powertrain, and accumulator (battery). The chassis is best viewed as the skeleton of the vehicle, tasked with functions of subsystem support, driver protection, absorption of forces, vibration damping and load distribution. It has many design requirements and specifications that inform its design. A preliminary representation of the work done this year on the entire Electric Vehicle project is provided below in Figure 1 as a reference.

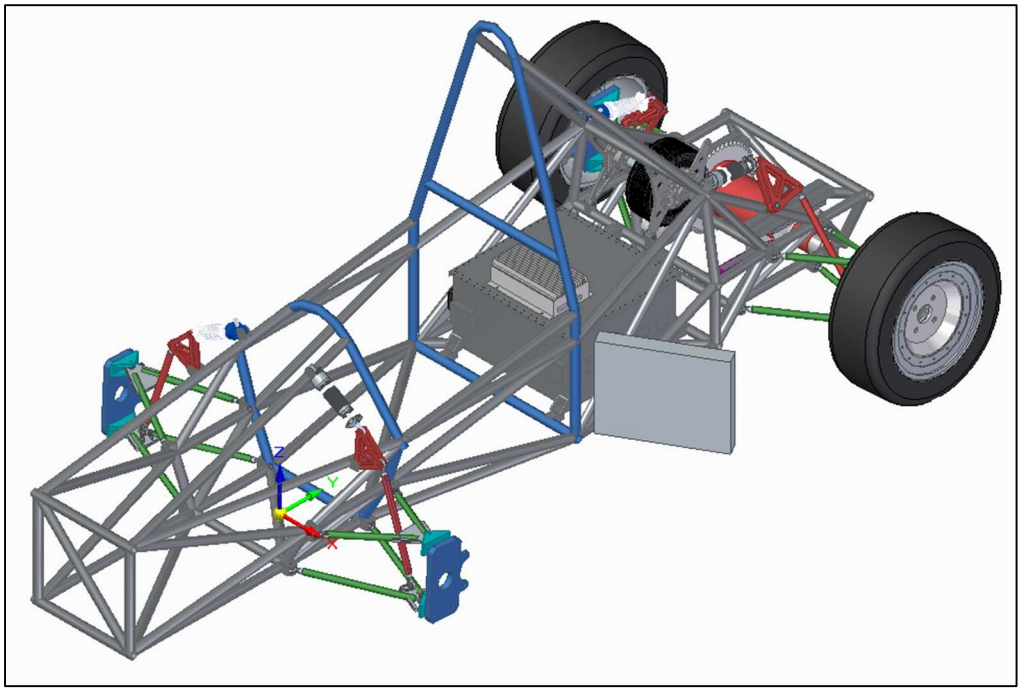

**Figure 1:** The Overall Electric Vehicle Designed by the Senior Design Team

The chassis team's job is to create a design that satisfies the FSAE requirements and serves the other subsystems in the most optimal manner. In conjunction with this, the role of the project explored in this paper is to use finite element modeling techniques and analysis to critically investigate and improve the structural properties of the chassis designs that are developed over the course of the EV Senior Design class. The final chassis design to be explored is shown below in Figure 2.

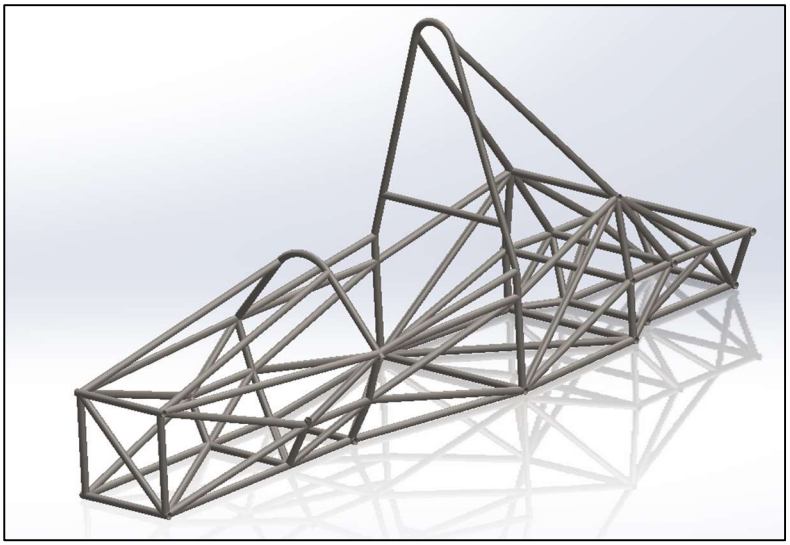

**Figure 2:** The Chassis to be Analyzed Over the Course of This Capstone Project

The physical version of this chassis after manufacturing is shown below in Figure 3.

**Figure 3:** Final Manufactured Chassis

The chassis shown in Figures 2 and 3 can be broken down into four distinct sections as shown in Figures 4 through 7 below. The organization of the chassis into sections will be useful for analyzing and determining which portions of the chassis need to be strengthened in later tests.

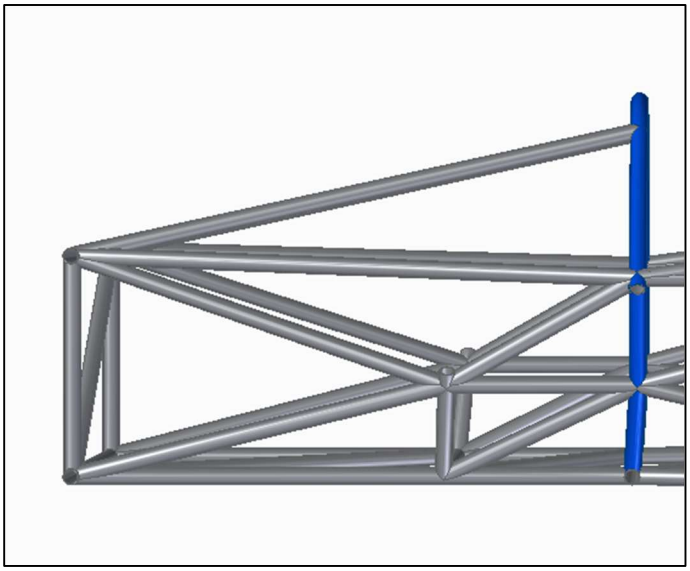

**Figure 4:** Front Section of the Chassis

Shown in Figure 4 is the first section of the chassis which spans from the front bulkhead to the front roll hoop. It contains the steering, front suspension, accelerator, brake, and driver's legs.

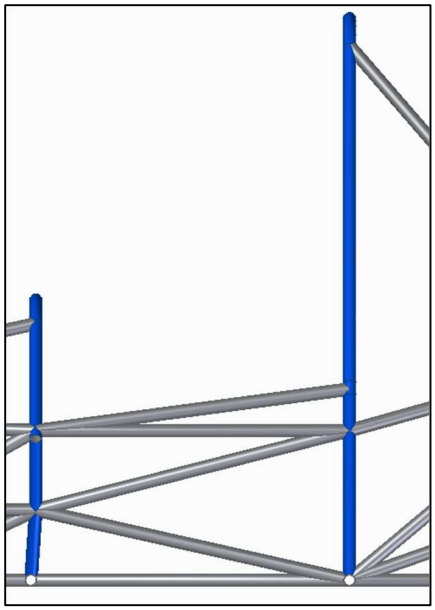

**Figure 5:** Side Impact Section of the Chassis

Shown above in Figure 5 is the second section of the chassis which connects the front roll hoop to the main roll hoop. This section is commonly known as the side impact structure and contains the seat and driver.

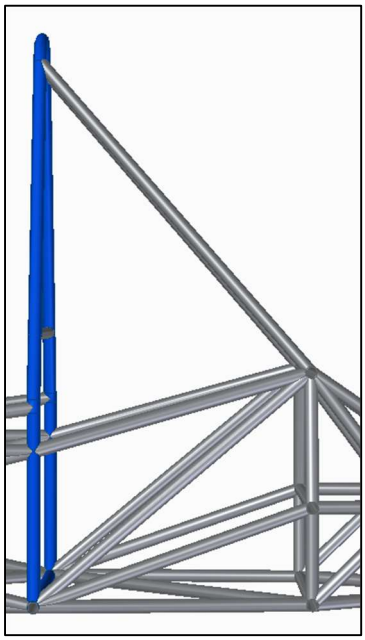

**Figure 6:** Accumulator (Battery) Section of the Chassis

Figure 6 above shows the third section of the chassis which connects the main roll hoop to the rear impact structure. This portion houses the accumulator and motor cooling components.

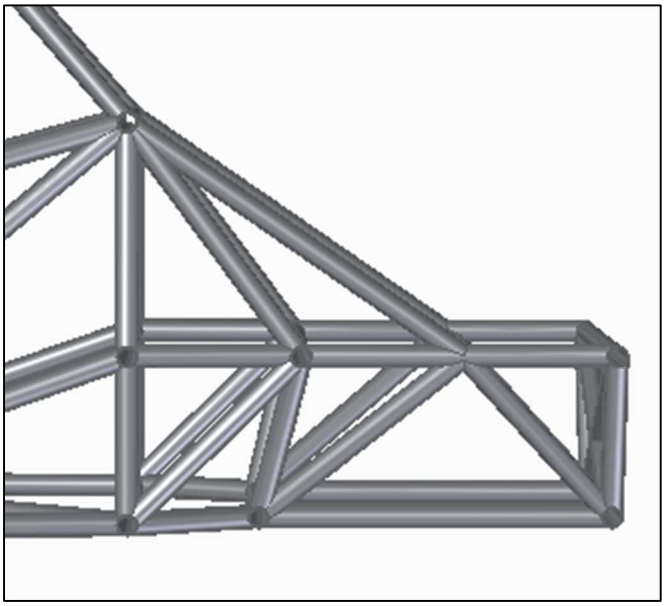

**Figure 7:** Powertrain Section of the Chassis

Finally, the fourth section of the chassis (Figure 7) spans from the rear impact structure to the rear of the chassis. It contains the powertrain components such as the motor, differential, axle, and drive chain, as well as the rear suspension components.

**Finite Element Analysis**

Finite Element Analysis (FEA) is a form of numerical method analysis that can be used to analyze and simulate engineering systems and real-world objects. Essentially, each system is divided into smaller and simpler elements where each element can be represented by a mathematical function. These functions can then be characterized by their properties and behaviors and turned into a system of equations that a computer can numerically solve. FEA can aid in predicting the behavior of systems too complicated to predict using hand calculations. It

can also be used to predict behavior under unique conditions and optimize designs. Stresses, strains, deformations, and other parameters can be analyzed by it. While Finite Element Analysis can be a very powerful tool, it is a simplified model of a real-world system. The accuracy of finite element models can be improved with experimental results that can be used to modify and calibrate the model. After the model is validated with experimental results it can then predict real life behavior with greater accuracy and confidence. One strategy to reduce the difference between the model's behavior and actual physical behavior is by reducing the size of the mesh's elements. Additionally, changing the element material properties, modifying the boundary conditions, and incorporating welded nodes improves the accuracy of the model. Overall, FEA is a powerful tool that can help engineers design and optimize complex systems, reduce development time and costs, and improve the performance and safety of engineered products.

**Overall Goals**

Overall, this capstone project will explore the usage of FEA to achieve the desired goals of the tube frame chassis design. Specifically, with each iteration we intend to determine structural properties such as torsional stiffness, and subsequently improve the chassis' behavior by the addition, subtraction, or redesign of various members of the chassis frame. The objective is to obtain a torsional stiffness of at least 1000 $\frac{N \cdot m}{degree}$, which is based on similar published FSAE chassis designs (Tripathi). Furthermore, an apparatus to physically test the structural properties of the manufactured chassis will be designed and fabricated. The FEA results and real-world test results will then be compared, and this comparison will allow for the confirmation of the computer models used.

## Torsional Stiffness as a Design Metric

### Theory of Torsional Stiffness

In order to better understand torsional stiffness, the theory and mathematics surrounding it must be examined. Torsion is the twisting of an object, for example a shaft, due to an external or applied torque. When torque is applied to a shaft, the shape of the shaft, its cross-sectional area, and the modulus of rigidity of the material will dictate the magnitude of twist for a given amount of torque. Circular shafts will have a lower angle of twist in torsion than a square shaft, all other factors being equal. This behavior is one of the main motivations behind the decision to use circular tubes instead of rectangular tubes to make the chassis frame. For a circular shaft, the torsional stiffness property is given below, where 'L' is the length of the shaft, 'G' is the shear modulus, and '$I_P$' is the polar moment of inertia:

$$Torsional\ Stiffness = \frac{G * I_P}{L}$$

While the individual stiffnesses for each member of the chassis could be calculated using that equation, in practice, because the chassis is more than just a single circular tube, it requires far more in-depth analysis to obtain a usable value for the torsional stiffness of the entire chassis. To calculate the stiffness of the entire chassis, the total amount of twisting along the length of the entire chassis is used. To find this total stiffness, the rear end of the chassis is fixed and one side of the front of the chassis is pinned. A fixed condition does not allow both rotation and translation, while a pinned condition does not allow translation. Next, a downward force is exerted on the side of the chassis opposite of the pinned side. This setup is similar to a scenario where one wheel hits a bump or load transfer occurs due to cornering, causing the chassis to twist. Figure 8 illustrates this concept below.

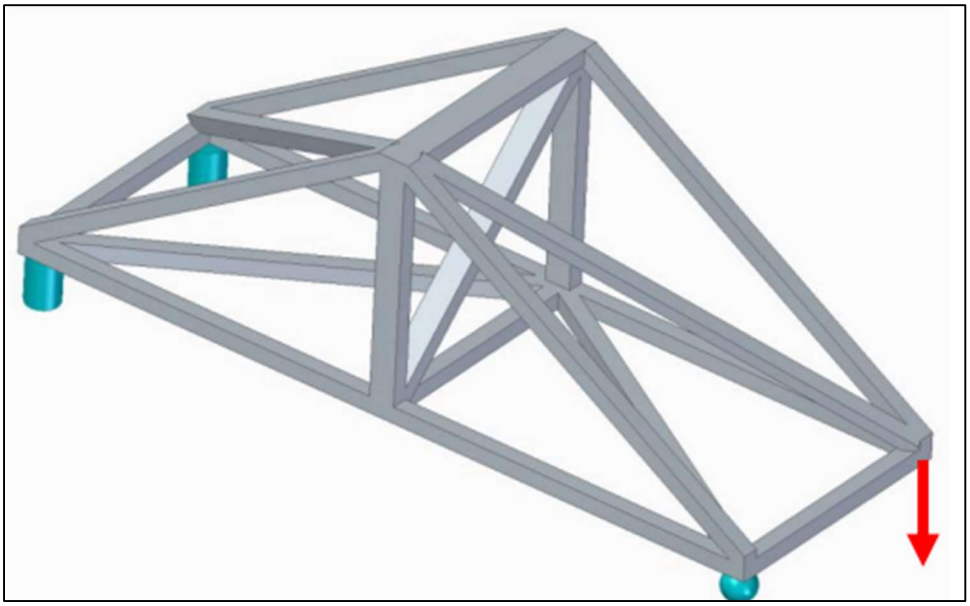

**Figure 8:** Illustration of Chassis Torsional Stiffness Setup

Once the chassis has been twisted as such, the overall deflection is measured. From this deflection and the knowledge of the length of the moment arm, the angle of twist of the chassis can be calculated as follows. This is where '$\theta$' is the angle of twist, '$\delta$' is the downwards deflection of the chassis due to the force, and 'L' is the length of the moment arm:

$$\theta = \tan^{-1}(\frac{\delta}{L})$$

In addition to the angle of twist, the total torque applied can be calculated by taking the downward force and multiplying it by the length of the moment arm. This is shown as follows where 'F' is the downwards force applied, and 'L' is the length of the moment arm:

$$Torque\ Applied = F * L$$

The moment arm is found to be the entire width of the chassis as the torque is causing rotation about the pinned location. For the most optimal analysis the torque should cause rotation about the center of the chassis, however, to keep the physical testing jig and the computer model consistent, rotation about the pinned point was chosen. From this applied torque and angle of

twist, the overall chassis torsional stiffness can be calculated by dividing the applied torque by the angle of twist. This will result in a total torsional stiffness value with units in $\frac{N \cdot m}{degree}$ for the chassis as follows where 'T' is the applied torque and '$\theta$' is the angle of twist of the chassis:

$$Torsional\ Stiffness = \frac{T}{\theta}$$

This torsional stiffness value will be used throughout to determine the structural properties of UAH's chassis and to compare it to reported values by other university teams. Chassis torsional stiffness greatly impacts the ride quality, the handling, the response to driver input, the functionality of the suspension, and the ability to tune the balance of the car effectively. Predictable handling can be best achieved if the chassis is stiff enough for it to be safely ignored.

**Benefits of Torsional Stiffness Comparisons**

Thinking of the chassis as a large spring connecting the front and rear suspension leads to the choice of mainly focusing on torsional stiffness. If the chassis has low torsional stiffness, attempts to control the load transfer by the driver will be confusing at best and impossible at worst (Milliken). When a vehicle turns or corners, its chassis is subjected to torsional loads due to the twisting forces that occur as the weight of the vehicle shifts from side to side. A chassis with low torsional stiffness will deform more easily under these loads, leading to a loss of stability and handling precision, and potentially compromising the vehicle's safety. On the other hand, a chassis with high torsional stiffness will resist these loads more effectively, maintaining the vehicle's stability and improving its handling characteristics.

Additionally, the torsional stiffness value of a chassis is a common metric that can be applied to multiple different chassis versions and types. This allows for a comparison with

various designs from both UAH's team and other universities' teams. It also allows for comparison over time with changing designs so correlations can be made with different teams at UAH.

For these reasons torsional stiffness was chosen as the primary comparison property for estimating chassis performance and evaluating iterative designs. This was selected as opposed to load testing, thermal testing, deformation, or stress testing which could have also been tested but played a minor role in the decisions of the UAH Senior Design EV Chassis team as a comparative tool. Thus, for each of the distinct chassis designs developed by the team, torsional stiffness properties were the primary point of comparison after other factors such as subsystem support and rules compliance had been met.

**Torsional Stiffness Benchmarks**

Since torsional stiffness is the primary property of comparison for the different chassis iterations, the question of benchmark values for chassis torsional stiffness must be addressed. To achieve this, the works of Satyam Tripathi and Hubbard Velie provide useful analyses into how idealized torsional stiffnesses affects the properties of FSAE racecars. Their separate analyses came to similar conclusions on the desired value for torsional stiffness, namely 1000 to 2000 $\frac{N \cdot m}{degree}$ (Tripathi; Velie). To support this point, a summary of the self-reported experimental torsional stiffnesses of various competitive universities was made in the table below where they were compared to the latest iteration of the chassis for UAH Senior Design EV team.

**Table 1:** Table of Torsional Stiffnesses of Competitive Teams

| **Reference** | **Torsional Stiffness ($\frac{N \cdot m}{degree}$)** |
|---|---|
| University of Akron | 1358 |
| University of Alberta | 1469 |
| University of Michigan | 2100 |
| University of Texas Austin | 2123 |
| 2021-2022 UAH Chassis | 1300 |
| Stated FSAE average (Tripathi) | 1500 |
| Hand-calculated average of chassis | 1525 |
| 2022-2023 UAH Chassis | 1503 |

From Table 1, on average most chassis tend to have a torsional stiffness above 1000 $\frac{N \cdot m}{degree}$, with some exceeding 2000 $\frac{N \cdot m}{degree}$.

In general, there are only three primary methods to increase torsional stiffness, each with its drawbacks. One way to increase stiffness is to increase the material modulus. However, in this instance the material is already set as 4130 Chromoly Steel based on the FSAE competition rules. Another route is to reinforce the entire structure by adding additional members or adjusting the geometry where multiple members meet. The drawback to this method is that it can add weight and complexity to the design's fabrication but overall, it has the greatest effect with a minimal drawback. Finally, the thickness of the tubes could be increased with the clear downside of directly adding weight. Principally, the weight of the chassis should be kept to an absolute minimum without sacrificing torsional stiffness. A weight which is too high could ultimately lead to a situation where the increased torsional stiffness does not justify the decreased handling, acceleration, and efficiency of the chassis. Clearly, there is a tradeoff between chassis torsional

stiffness and chassis weight, so the chassis' stiffness cannot simply be increased indefinitely. Using torsional stiffness will ensure that the decisions made are informed by a sufficient body of evidence, which enables the improvement of the performance of the UAH Senior Design FSAE Vehicle.

**Physical Illustrations of Tests of Torsional Stiffness**

The experimental measurement of a chassis is a technical process. In effect it involves constraining the chassis' rear pivots, which are preferably suspension mounts, to a rigid frame using clamps, bolts, or other means. It is important to ensure the frame itself is strong enough to not fail during the test. Next a torque is applied to the chassis in some way, usually though a moment arm or a hydraulic actuator. This induces deformation in the chassis frame, which in turn leads to twisting. The deformation of the chassis is measured at several points using displacement sensors. It can also be measured by attaching strain gauges to the chassis. From this, the torsional stiffness can be calculated, and the results analyzed to determine if the chassis meets the required stiffness specifications (Riley; Kaneb). An example of this setup is illustrated in Figure 9 below.

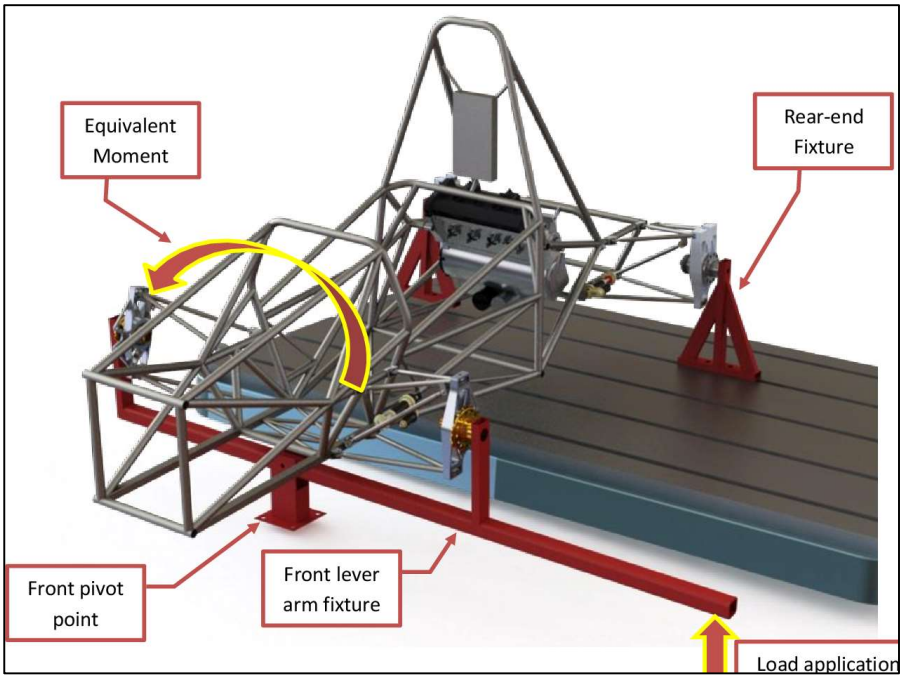


**Figure 9:** CAD model of experimental setup for The Cooper Union for the Advancement of Science and Art (Chambers et al.)

Often, the setup of the jig varies from vehicle to vehicle, depending on the needs and capabilities of the specific organization or engineering team. In Figure 9 above, an example of the torsional test rig for the Cooper Union for the Advancement of Science and Art FSAE vehicle is shown. In the CAD model, it is easy to observe which points on the chassis have been chosen as pivot points for mounting the chassis onto a frame and an example of this mounting after manufacturing is shown in Figure 10 below.

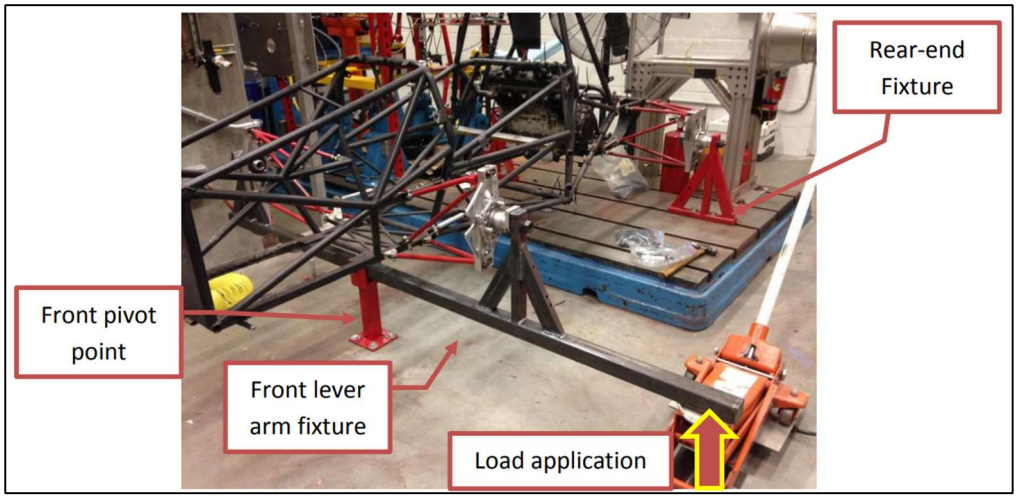


**Figure 10:** Real World Assembly of Torsional Stiffness Testing Rig (Chambers et al.)

Figure 10 shows the real-world assembly of the torsional test rig modelled in Figure 9. Another example, shown in Figure 11, depicts a torsion testing jig from the University of Michigan which added solid springs and decided to apply the load in the opposite direction. For each team, the procedure for conducting a test is consistent leading to little variation in thoroughly conducted tests. This offers a reliable and easy comparison between different vehicle chassis that can inform design considerations.

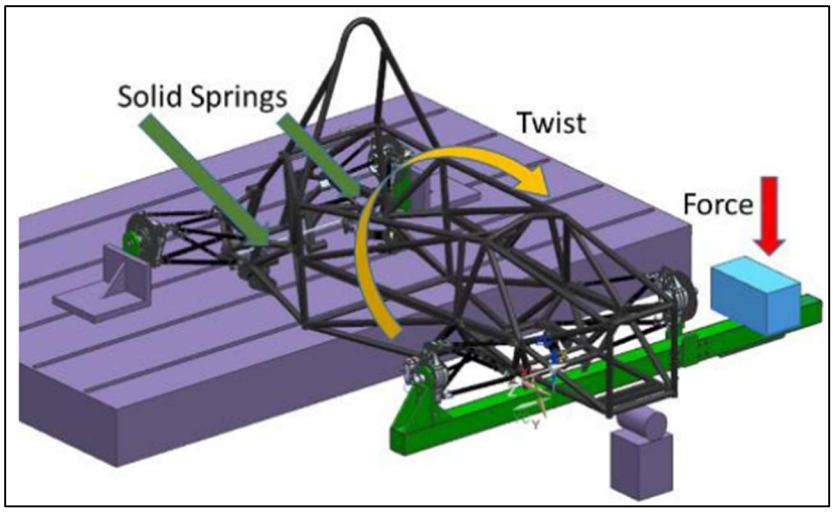


**Figure 11:** CAD model of experimental setup for The University of Michigan (Milliken)

## Finite Element Analysis

### Torsional Stiffness Model Setup

Finite Element Analysis (FEA) is the optimal method for analyzing the torsional stiffness before manufacturing a chassis. It enables the comparison of each new version of the chassis to the previous one without needing to manufacture a physical version of every chassis design. For the FEA, once the chassis is appropriately constrained, a force is applied at a specific location to elastically deform the chassis in a twisting scenario. When performing the FEA for this project, the chassis was constrained as shown in Figure 12 below. The FEA was performed in both Solid Edge and SolidWorks using a linear static beam analysis. This equates to an analysis where the appropriate tube cross sections connect each node.

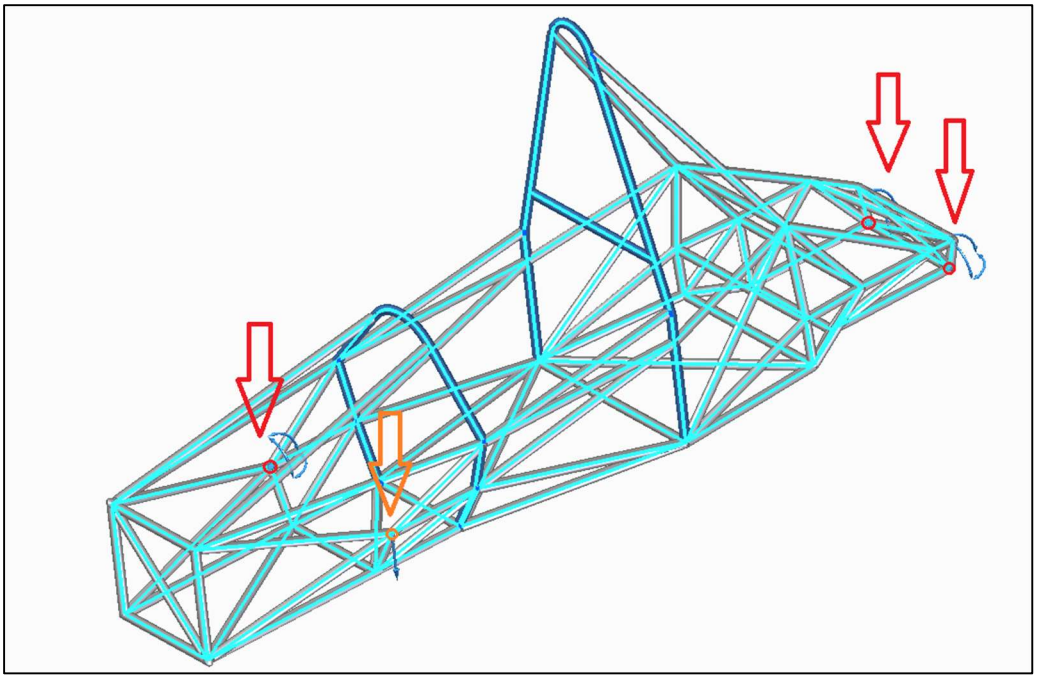

**Figure 12:** FEA setup for testing Torsional Stiffness

As can be seen in Figure 12, the rear of the chassis is fixed at the red circles, while the red node at the front of the chassis represents a pinned condition. This means the front pinned node cannot

translate but can still rotate. A downward force of 1000 Newtons is then applied at the orange node which is the other suspension mounting point. From these forces the chassis twists about the one suspension mounting point that is pinned. As previously detailed, to find the torque applied to the chassis, the 1000 Newton force is multiplied by the moment arm length which is the distance between the two suspension mounting points. After calculating the torque, the degree of twist can be found by taking the amount of vertical deflection that the orange node experiences and using it to calculate the angle of twist. A torque and angle of twist value are then used to calculate an overall torsional stiffness value. An illustration of the results of an FEA simulation are shown below.

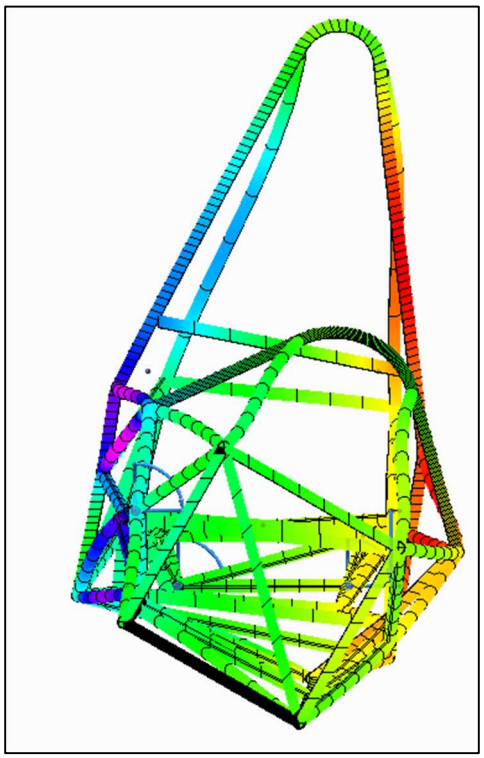

**Figure 13:** Example FEA Result

The result in Figure 13 showcases the output that each FEA model produces. There is both a physical deformation aspect where the clockwise twisting can be seen, and a color gradient

aspect where specific shades can be matched to the appropriate value on a legend. In this case the output was displaying the degrees of twist for each portion of the chassis mesh.

**Results of the FEA for the Design Iterations**

As detailed previously, the overall torsional stiffness of each chassis version was calculated and can be compared to each other. This analysis was run on every version of the Senior Design team's chassis and summarized along with a chassis weight and chassis member count. Shown in Table 2 below are the results for all the chassis designs up until the final production version, V7.3.3, along with the change that accompanied each version in order to have a better understanding of how the torsional stiffness was affected. These different changes and variations will be examined in detail following Table 2.

**Table 2:** Summary of FEA Results for Each Chassis Version

| *Chassis Version* | *Vertical Displacement (mm)* | *Torque (N*m)* | ***Torsional Stiffness*** $(\frac{N \cdot m}{degree})$ | *Chassis Weight (lb)* | *Chassis Members* | *Main Change* |
|---|---|---|---|---|---|---|
| V5.2 | 6.105 | 620 | **1099** | 86.8 | 83 | Simplified suspension |
| V5.3 | 6.965 | 620 | **963** | 85.2 | 80 | Reduced rear box |
| V5.3.2 | 6.61 | 620 | **1015** | 85.2 | 80 | Fixed triangulation |
| V5.3.3 | 5.22 | 620 | **1285** | 90.6 | 85 | Tested extra bracing |
| V6 | 4.235 | 510 | **1072** | 90.2 | 90 | Finalized sub team interactions |
| V6.1 | 3.835 | 510 | **1184** | 90.7 | 90 | Fixed rear axle |
| V6.2 | 4.15 | 510 | **1094** | 90.8 | 90 | Fixed differential interference |
| V6.3 | 3.66 | 510 | **1240** | 98.6 | 92 | Modified based on analysis |
| V7.3.3 | 3.02 | 510 | **1503** | 103 | 93 | Adjusted rear of chassis to accommodate sub teams and revised for manufacturing |

The versions of the chassis preceding version V5.2 were not analyzed using FEA because until that point the general shape of the chassis was still forming, and analysis was not required. To arrive at the torsional stiffness values listed in the table above, the stiffness of the chassis when twisted in each direction was calculated. These two stiffness values were then averaged together to account for any non-symmetry in the chassis design and arrive at the overall stiffness listed. For most of the versions prior to V6.2, the chassis was changed to meet the requirements of a design sub-team and then an analysis was performed on it. Because of this, it was mostly a reactive analysis as opposed to an analysis with the intent to improve the design. However, once

the team reached V6.2, the chassis for the most part conformed with all the other design sub-systems so future versions had the specific intent to improve the torsional stiffness. The overall stiffness values from V5.2 to V6.2 were essentially the same as they were 1099 $\frac{N \cdot m}{degree}$ and 1094 $\frac{N \cdot m}{degree}$ respectively.

The first analysis that was performed on V6.2 was regarding the lack of a cross member underneath the accumulator (battery) compartment. This compartment was contained in the third section of the chassis shown previously in Figure 6. The accumulator was originally planned to be removed through the bottom of the chassis so a cross member underneath it could not be added. However, this method of removal was changed to allow the accumulator to be removed through the driver's compartment so a cross member could now be added back into the chassis if needed. FEA was performed on V6.2 without the cross member to determine if it would be beneficial to add one. The results are illustrated in Figure 14 displaying displacement below.

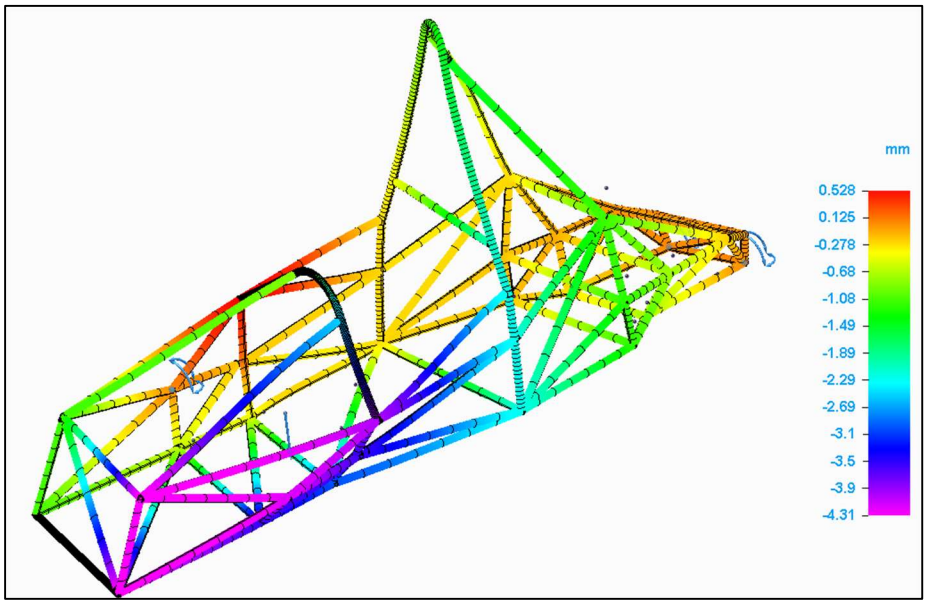


**Figure 14**: FEA of V6.2 Without Accumulator Cross Bar

As can be seen from Figure 14 showing the vertical displacement of the chassis, the rear end of the accumulator compartment has a significant amount of displacement. This analysis led to the decision to add the cross member back into the chassis. Adding it back in created the following chassis design.

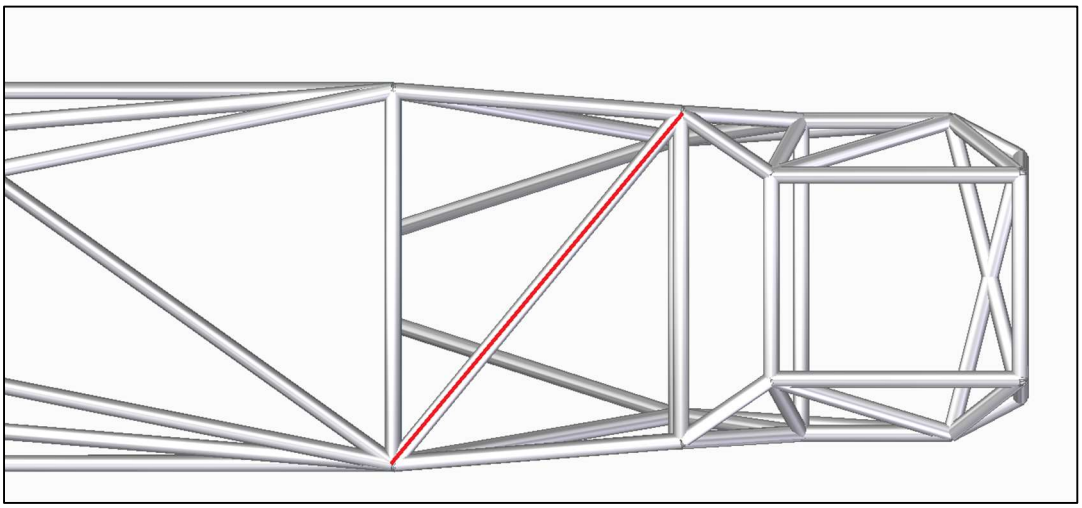

**Figure 15:** Bottom View of Chassis with Added Cross Member Shown in Red

The cross member that was added back into the chassis is shown in red in Figure 15. Adding this cross member increased the chassis weight by only 1.61 pounds and provided an increase in torsional stiffness of 65 $\frac{N \cdot m}{degree}$. Additionally, it provided support for the accumulator to rest on.

The next technical analysis that was performed on V6.2 pertained to the strength of the side impact structure. The side impact structure spans the length of the second section of the chassis and was shown in Figure 5 previously. After analyzing V6.2 and looking at a plot of the degrees of rotation about the longitudinal axis it is clear that the side impact structure is the source of the most twisting of all the major sections of the chassis. This can be seen below in Figure 16 displaying degrees of rotation where red represents the most rotation.

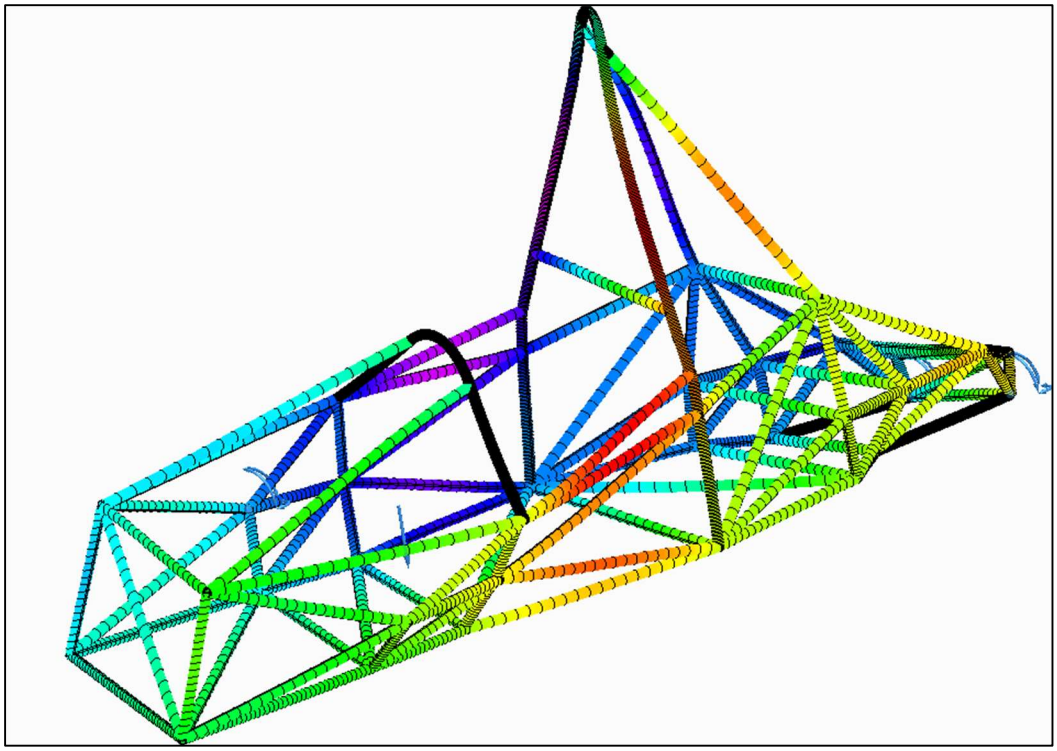

**Figure 16:** FEA of Chassis Showing Degrees of Rotation About the Longitudinal Axis

This plot shows the rotation about the longitudinal axis. The side impact structure of the chassis is shown in red meaning that the most twisting is occurring there. This analysis indicated that the side impact structure should be improved. To do so, better triangulation was used in this structure to improve the stiffness. A before and after view of the side impact structure is shown below in Figures 17 and 18.

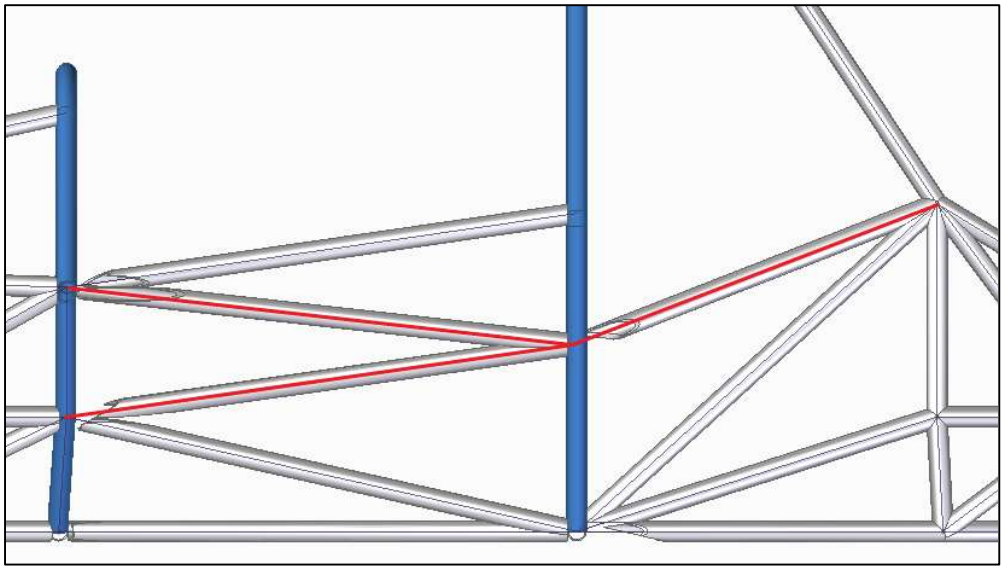

**Figure 17:** Side View of Side Impact Structure in V6.2 (Before)

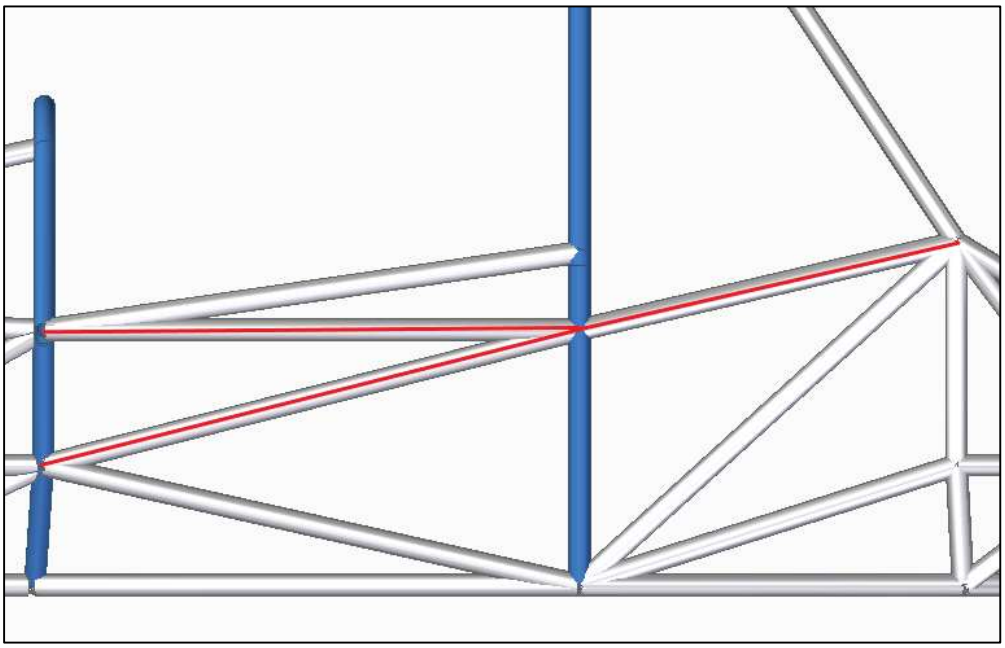

**Figure 18:** Side View of Side Impact Structure in V6.3 (After)

From V6.2 to V6.3, as shown in Figures 17 and 18 respectively, the triangulation was improved. This resulted in the members being collinear and allowing the load path to be improved, thus improving the torsional stiffness. This change did not increase the weight of the chassis and it

improved torsional stiffness by 75 $\frac{N \cdot m}{degree}$ while also still meeting the rules for the side impact structure layout detailed in the FSAE rule F6.4.4. A FEA analysis of V6.3 shown below also illustrates the chassis improvements to overall twisting due to these analysis items.

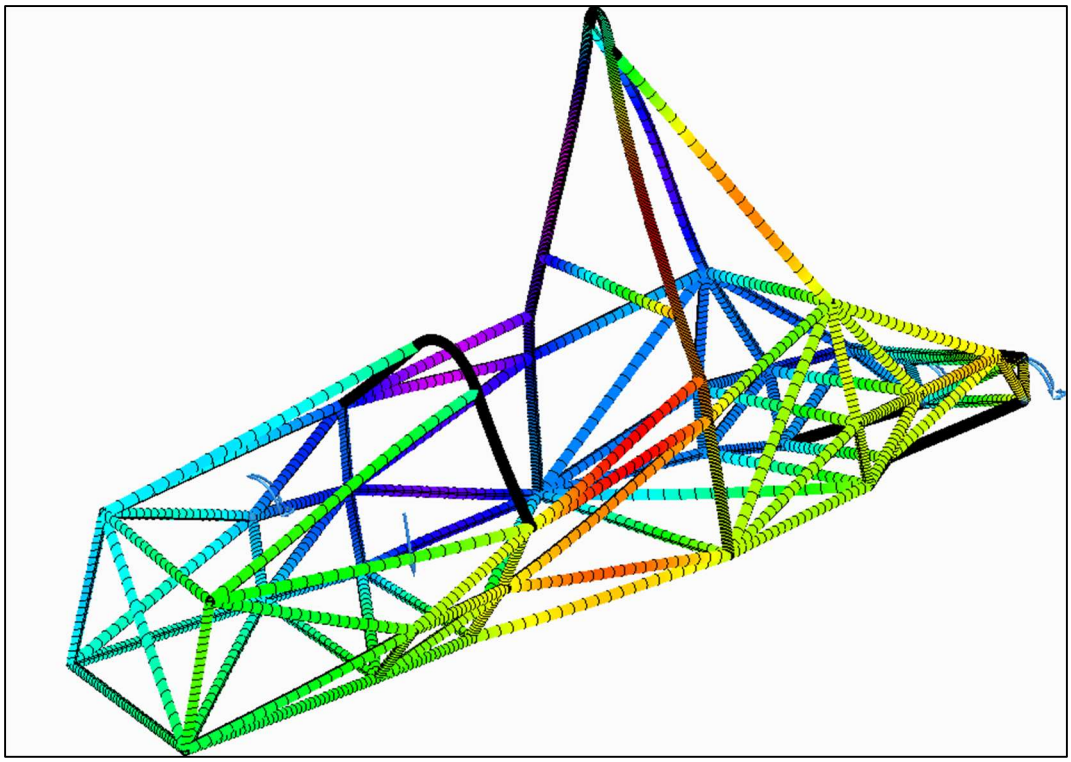

**Figure 19:** FEA of Chassis V6.3 After Improving Side Impact and Adding Cross Member

In the end, both technical analysis items improved the torsional stiffness of the chassis by 150 $\frac{N \cdot m}{degree}$ combined. After two technical analysis cases, the torsional stiffness went from 1090 $\frac{N \cdot m}{degree}$ in V6.2 to 1240 $\frac{N \cdot m}{degree}$ in V6.3.

At this time, it was determined that for future designs the side impact structure seemed to be the location needing the most improvement. Because of this, a potential improvement was also analyzed where the side impact tubes were changed from Type B tubing to a thicker Type A tubing. This change meant the tubes went from a wall thickness of 0.65 inches to 0.95 inches.

After performing this analysis, the stiffness was improved by an additional 100 $\frac{N \cdot m}{degree}$, but it also increased the weight of the chassis by ~10 pounds. This increase in stiffness was not deemed to be worthwhile when compared to the weight increase it would cause. Other possible additions to the side impact structure involved adding tubing members for more support. However, since the chassis member count was already at 92 this decision was not chosen.

From V6.3 to the final version, V7.3.3, the focus was turned away from the side impact structure and towards the rear of the chassis. The first change investigated adjusted the previously angled end of the chassis to be square. This change is shown in Figures 20 and 21 below where the new design is in silver, and the previous design is in blue. Red lines indicate more clearly the previous angles.

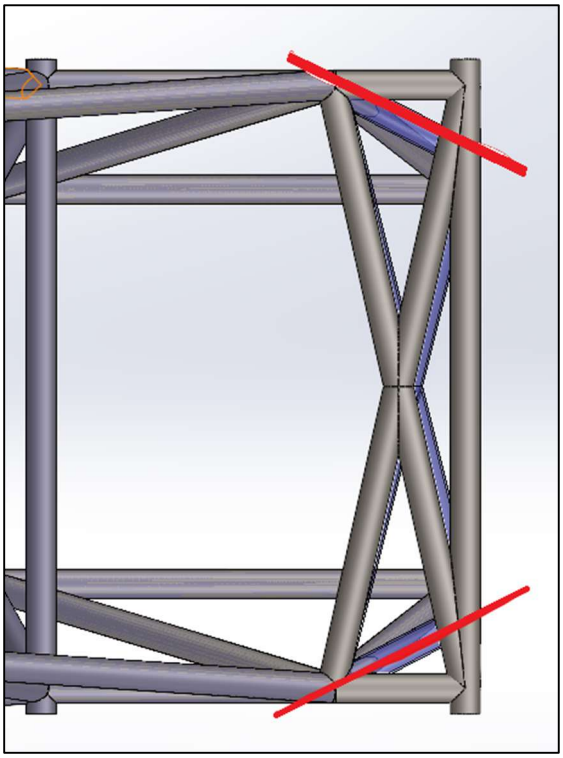

**Figure 20:** Squaring Out the Rear of the Chassis Top View

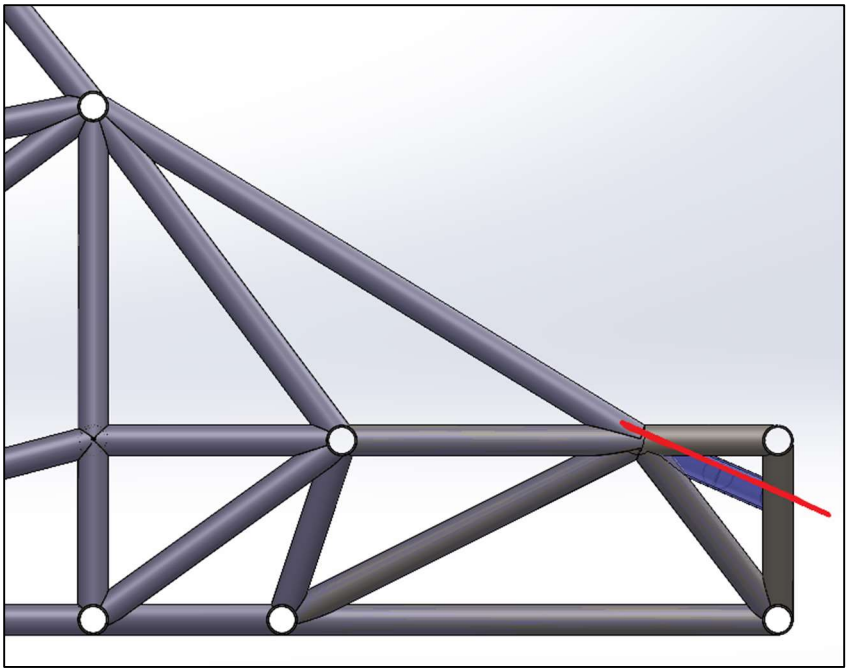

**Figure 21:** Squaring Out the Rear of the Chassis Side View

The squareness from the new design helped to triangulate the forces better throughout the chassis. This consequently helped to improve torsional stiffness. In addition to this change, the rear of the chassis was expanded in size. This modification is illustrated in Figure 22 below.

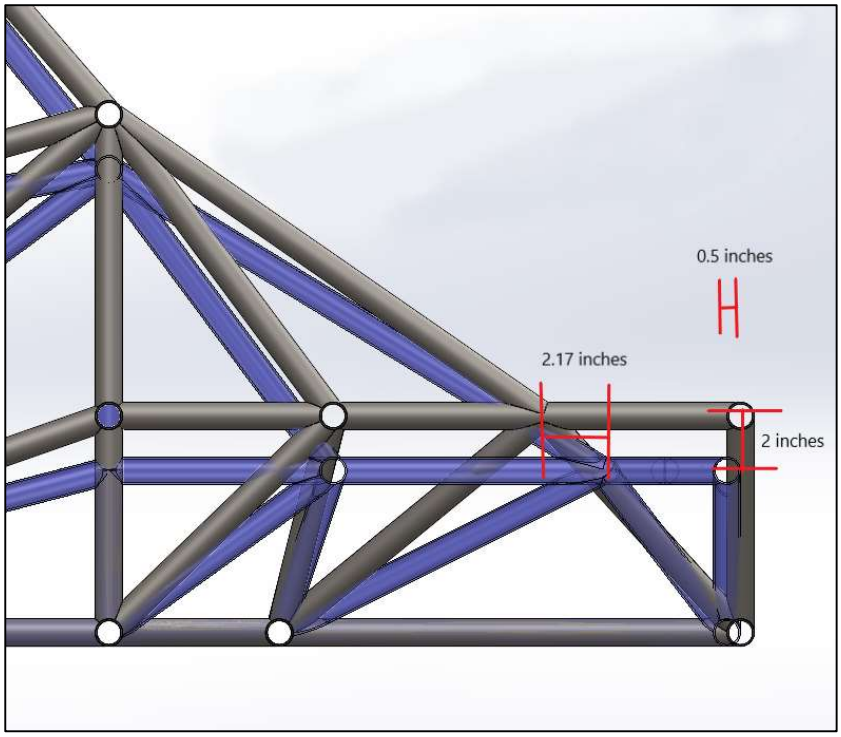


**Figure 22:** Expanding the Rear of the Chassis

Figure 22 shows a comparison between versions where the new chassis design is shown in silver and the old design is shown in blue. This change raised the chassis by 2 inches, extended the length by 1/2 of an inch, and adjusted the triangulation of a node by 2.17 inches. The main contribution to higher torsional stiffness was the more linear triangulation caused by moving the node 2.17 inches. Additionally, a few tubes where the suspension mounts to the chassis were thickened from 0.65 inches to 0.95 inches of wall thickness. Finally, all the end conditions where tubes meet each other were revised and finalized for manufacturing, which resulted in a more accurate model. The FEA model of the final version, V7.3.3, is shown below in Figure 23.

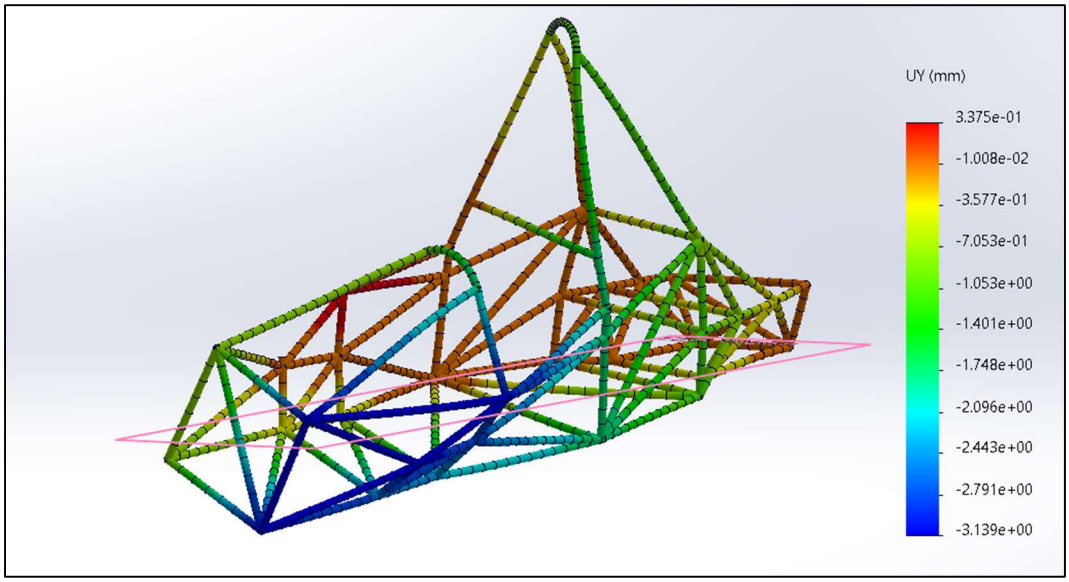


**Figure 23:** V7.3.3 Final FEA Results

For this final analysis in Figure 23, a vertical displacement of 3.02 millimeters was measured. This resulted in an overall increase in torsional stiffness of 263 $\frac{N \cdot m}{degree}$ from V6.3 to V7.3.3. This increase caused only a ~4.5-pound increase in weight and only a 1-member increase in total chassis members. As is summarized in Table 2, the final torsional stiffness value calculated was 1503 $\frac{N \cdot m}{degree}$.

From the first version analyzed to the final version, the chassis gained 404 $\frac{N \cdot m}{degree}$ in torsional stiffness. This 36.8% increase from 1099 $\frac{N \cdot m}{degree}$ to 1503 $\frac{N \cdot m}{degree}$ was achieved over the course of the year. At the same time, the weight of the chassis increased from 86.8 pounds to 103 pounds, which is only an 18.7% increase. This shows the torsional stiffness was successfully increased while maintaining a less significant impact on the weight of the chassis. The chassis exceeds its initial design goals and illustrates how FEA can aid in optimizing the physical performance and behavior of a complex structure.

## Physical Testing

### Torsional Stiffness Jig Design

Until this point, all the torsional stiffness calculations and values were purely based on theoretical models. Ideally, a physical version of the chassis would be tested and the values from these experimental tests would be compared to the computer models. To physically test the torsional stiffness of the chassis, a torsion jig was designed, manufactured, and used over the course of this capstone project. In the earlier section of this report on examples of real-world torsion jigs, some torsional testing devices built by other teams and companies were shown. Most of these devices use pivot mechanisms and sliders while attaching to the suspension uprights to provide the most accurate measurement of torsional stiffness. In the case of this capstone, due to limited resources and time, a modified torsional jig that matches the procedure of the FEA analysis was designed. To summarize the method, three points on the chassis are pinned, and a force is applied to a fourth point to cause twisting of the chassis. The design of the torsional testing setup is illustrated in Figure 24 below.

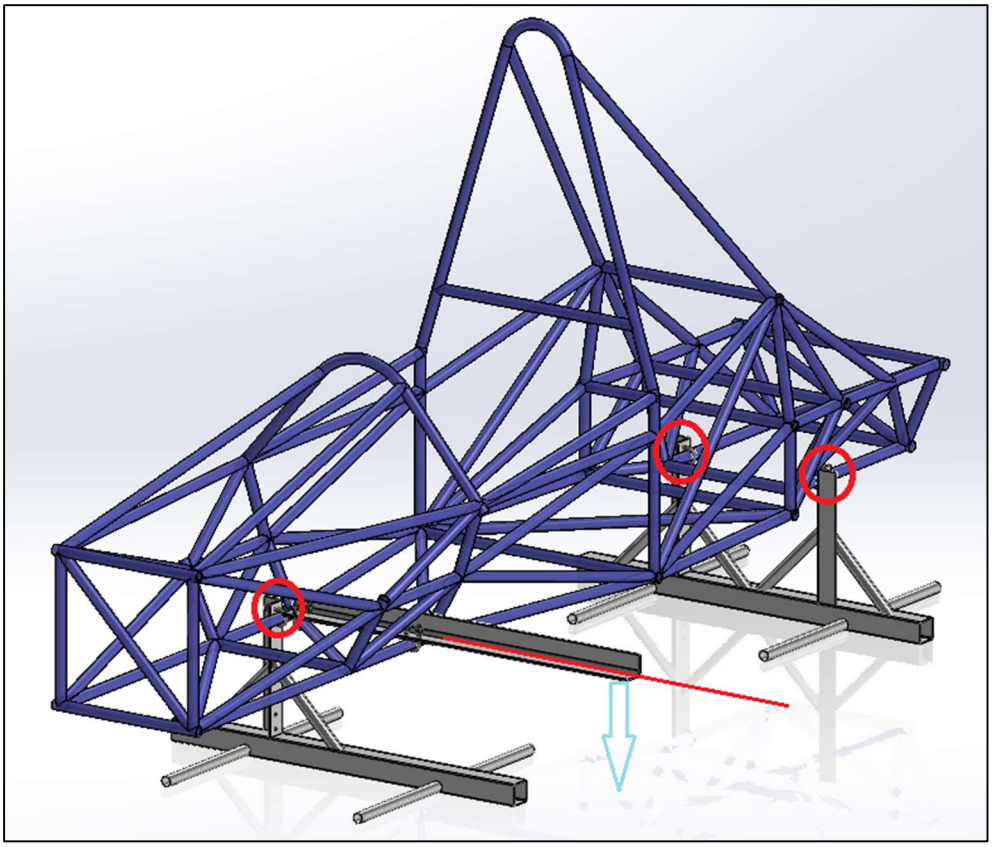

**Figure 24:** Overall Torsional Testing Rig

In Figure 24 the chassis, shown in blue, is secured to the torsion rig at the three suspension mounting locations circled in red. A laser is mounted on the moment arm illustrated by the red line and the measurement of the change in position of the projected laser spot onto a vertical surface due to the applied load on the moment arm allows the vertical displacement of the chassis to be measured. This approach of utilizing a moment arm and laser allows for the easy measurement of a small amount of deflection such that less force can be applied to the chassis. Hung on the moment arm is a weight that causes the chassis to twist about the front pinned node. This applied weight is represented by the blue arrow. Knowing the applied weight, the length of the moment arm, and the vertical displacement, the overall chassis stiffness can be calculated

using the previously detailed equations. Each of the components for the overall jig along with additional supports and stiffeners will be detailed below.

Firstly, the rear portion of the torsion jig is shown below in Figure 25.

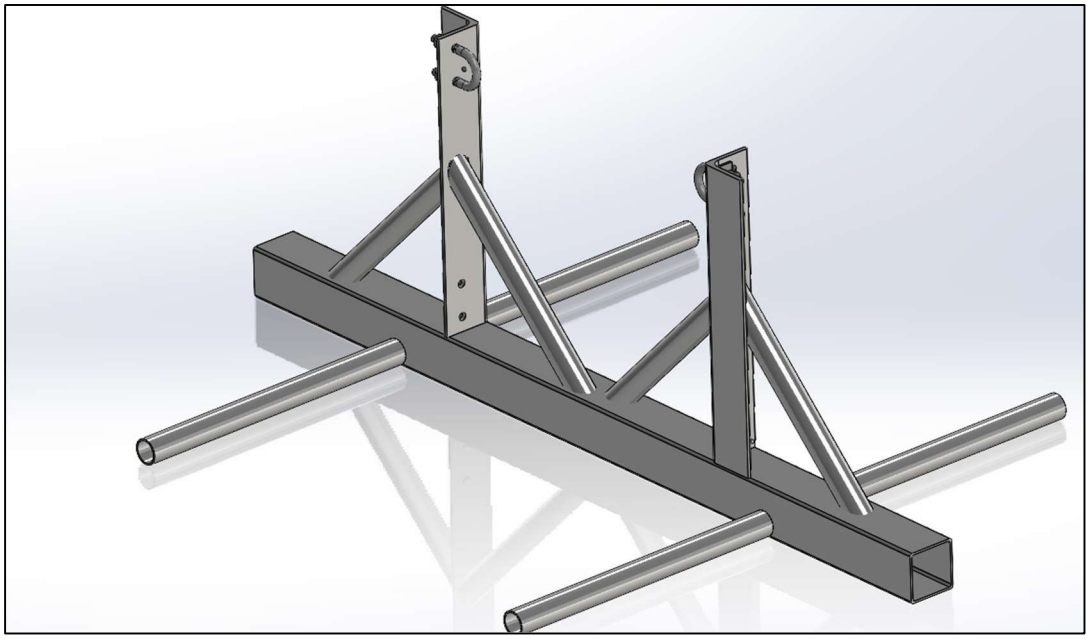

**Figure 25:** Rear Portion of Torsion Jig

The main structure of this portion of the testing apparatus is a 3-foot long, 2-inch by 2-inch square tube with two pieces of 1-foot long, 2-inch by 2-inch angle stock welded vertically to it. Both components are made from low-carbon steel. Connected to the angle stock are two U-bolt brackets that will secure the chassis in place. Joining the angle stock and square stock at a 45-degree angle are round tubes used to brace the entire structure. Protruding perpendicular to the square tubing, round tubes are welded on that will provide additional support, stability, and allow the entire jig to be mounted to a rigid welding table. These rounds tubes were chosen because there was excess left over from a previous UAH Senior Design team. Shown below is a close-up view of the rear portion of the jig connected to the chassis, where the chassis is modeled in blue for clarity.

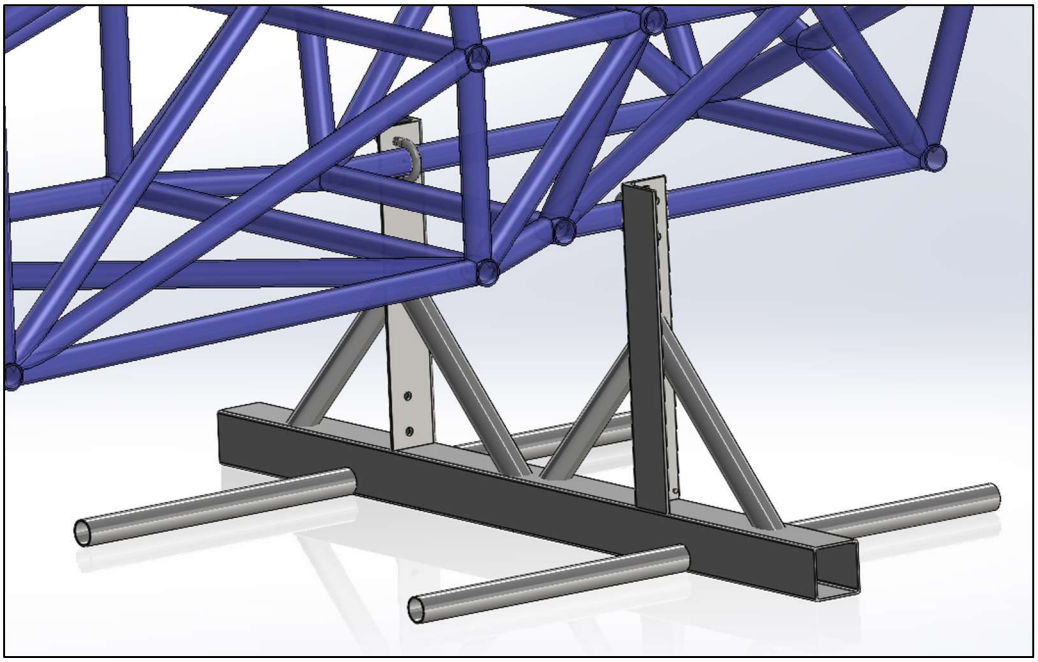

**Figure 26:** Integrated Rear Portion of Chassis

This rear portion can be slid as close to the node where the tubes join as possible. This will help prevent damage to the chassis, as well as aid in simulating a more realistic torsional jig setup by pinning the chassis close to where the suspension mounts to the chassis.

Moving to the front of the chassis, the system containing the front testing structure and the moment arm is shown below in Figure 27.

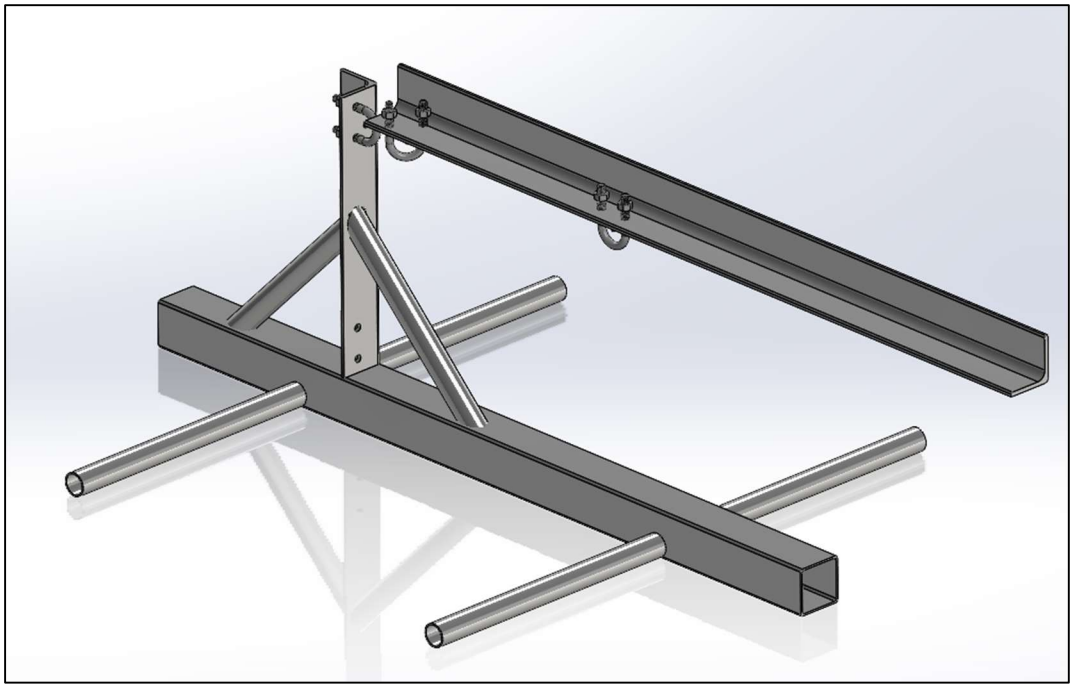

**Figure 27:** Front Portion of the Torsional Jig Assembly

Similar to the rear, the angle stock is welded vertically to the rectangular tubing. A U-bolt is also connected, and round tubes are welded for support. Also shown in this assembly is the moment arm where the twisting action will be applied to the chassis. This is made from low-carbon steel and is a 3-foot piece of 3-inch by 2-inch angle stock. This moment arm attaches itself in two separate places to ensure a rigid fit. A notch was machined near the end of the moment arm so a weight can be hung to provide the torque. A laser will also be mounted on the end of the arm to allow for easier measurements of small displacements. Shown below in Figure 28 is the front portion of the torsion jig attached to the chassis, where again the chassis is shown in blue.

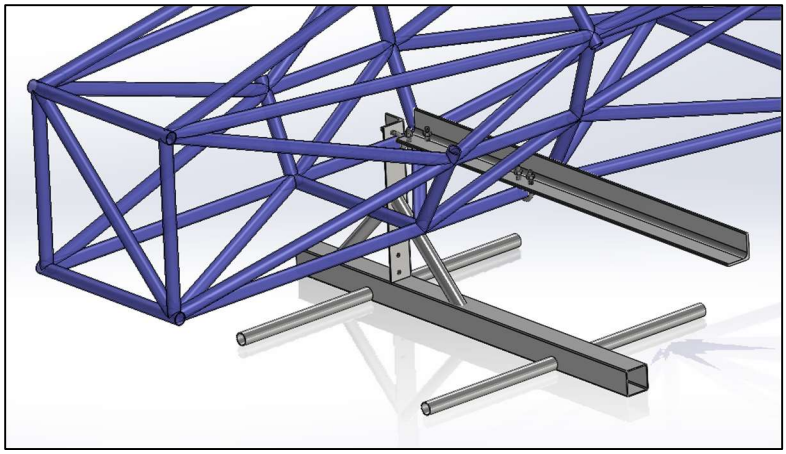

**Figure 28:** Integrated Front Portion of Chassis

The positioning of this front system can also be adjusted prior to installation. The entire setup was bolted down to a welding table at UAH's machine shop. Below, Figure 29 represents what this entire setup looks like with the chassis being shown in blue and the acorn welding table shown in orange.

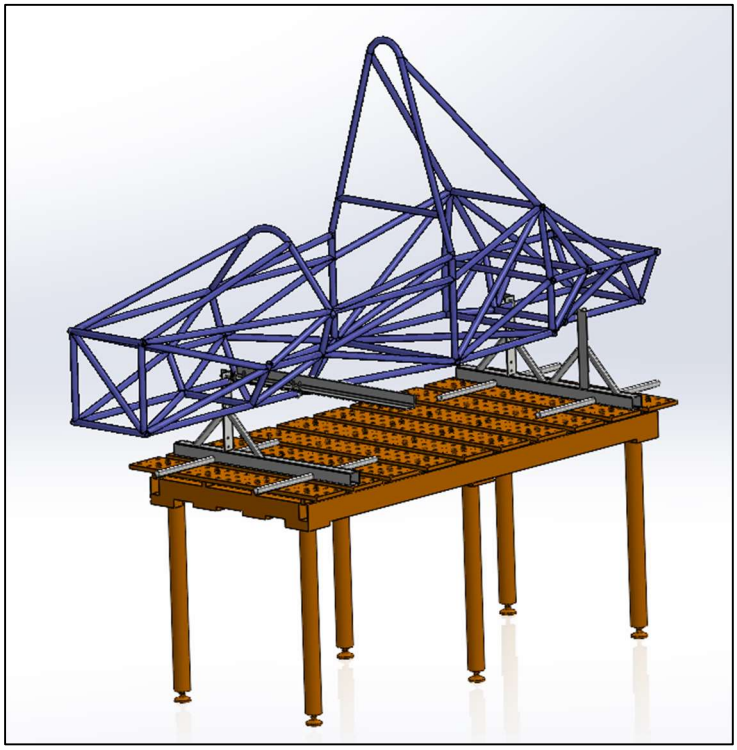

**Figure 29:** Complete Testing Setup

**Torsional Stiffness Testing**

The design for the torsional stiffness jig explored previously was fully manufactured and integrated with the chassis during this capstone project. The torsional stiffness jig is pictured below in Figure 30. It represents the designs shown in Figures 25 and 27.

**Figure 30:** Manufactured Torsion Testing Jig

Seen in Figure 30, the torsion testing jig that was manufactured accurately matches the intended design. In order to test the chassis' torsional stiffness and measure values to compare to the FEA, the jig had to be secured to a table and connected to the chassis in a way similar to what was shown in Figure 29. Below, in Figures 31 and 32, this complete testing setup is shown.

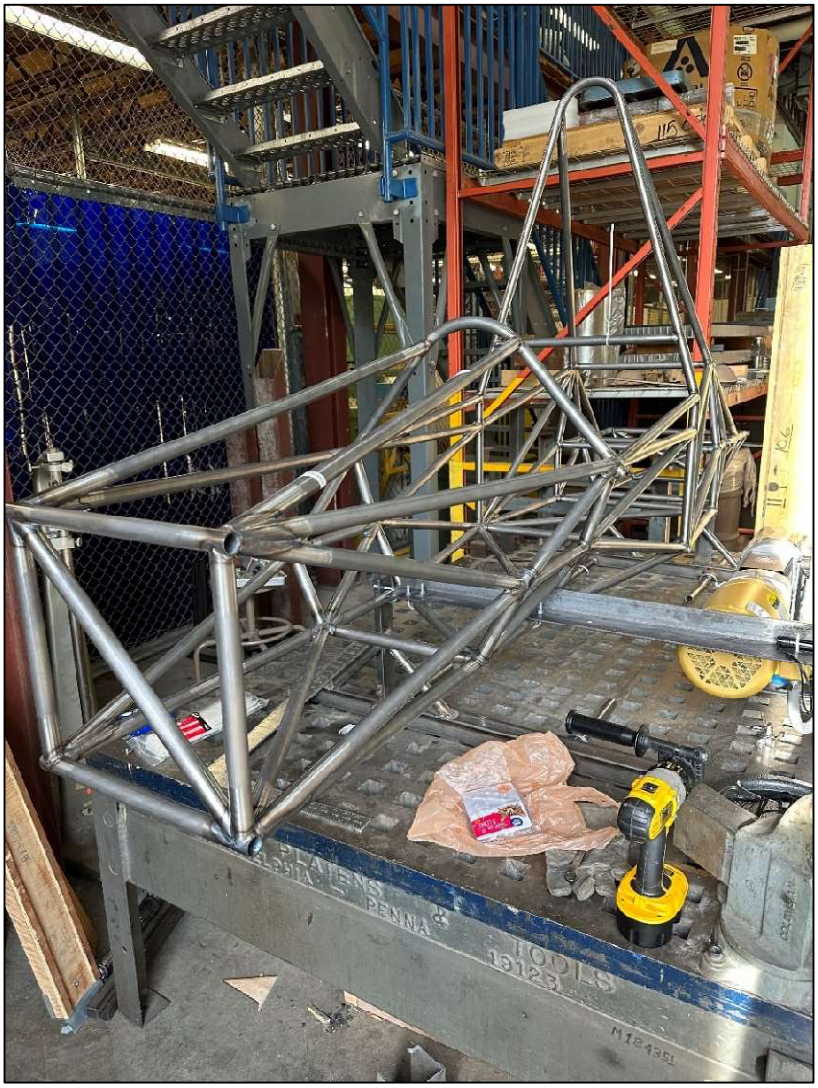

**Figure 31:** Complete Torsion Testing Setup

**Figure 32:** Complete Torsion Testing Setup

As shown above, the entire system functioned as designed and was constrained in the locations highlighted in Figure 24. The components of the testing jig were connected to the chassis and the jig was securely bolted to the acorn welding table with U-bolts. With the chassis attached to the torsion testing system, tests were conducted to provide experimental torsional stiffness values. These torsional stiffness values were the first indications of the true structural behavior of the final manufactured chassis outside of computer simulations. A total of 13 tests were conducted

using four different applied weight amounts. These tests were performed as outlined in the previous section on the design of the torsion testing jig. In this case, the length of the moment arm used was 0.98 meters. Table 3 summarizes these tests and shows the average values for each weight category that was tested on the chassis.

**Table 3:** Results from Physical Torsional Testing

| *Force Applied (N)* | *Average Angle of Twist (°)* | *Torque (N*m)* | *Average Torsional Stiffness* ($\frac{N \cdot m}{degree}$) |
|---|---|---|---|
| 120.10 | 0.08179 | 117.45 | 1442 ± 95 |
| 150.10 | 0.11052 | 146.79 | 1328 |
| 198.24 | 0.14000 | 193.86 | 1392 ± 104 |
| 209.07 | 0.17684 | 204.45 | 1156 |

The final average of all the tests performed on the chassis was 1360 $\frac{N \cdot m}{degree}$. The expected torsional stiffness of the chassis from running FEA calculations detailed previously was 1503 $\frac{N \cdot m}{degree}$. This is a 10% difference between the actual and expected torsional stiffness values.

While a smaller difference would be ideal, a 10% difference indicates the model and the manufactured chassis behave reasonably similarly. Some of this 10% discrepancy is because the torsion jig does not attach to the chassis exactly at a node where chassis tube members meet. The FEA model uses the center of a node to position its analysis, while the physical jig is slightly offset from these nodes. A large portion of the remaining 10% difference can be attributed to experimental error. When measuring the displacement of the chassis to calculate the stiffness, a change of even 1/32$^{nd}$ of an inch drastically alters the torsional stiffness values. 1/32$^{nd}$ of an inch specifically corresponds to a ~325 $\frac{N \cdot m}{degree}$ change on average, which is larger than the entire

difference between the expected value and experimentally measured value. Due to the diameter of the laser dot used and the precision of the measuring equipment available, the confidence of our displacement measurements only lies at around ±1/32nd of an inch. With this amount of error, the experimentally calculated result for torsional stiffness of 1360 $\frac{N \cdot m}{degree}$ certainly falls within the expected range and validates the FEA models, thus satisfying the second goal of this capstone project.

Because of the potential experimental errors experienced with this current approach, we recommend that future teams expand on the torsional testing jig setup to reduce this error. Teams with more resources to devote to the torsion testing system should consider using a more traditional setup as shown in the section on torsional stiffness benchmarks. The ideal system would consist of a pivoting system attached to the vehicle's suspension uprights that utilizes springs and sliding mechanisms. This setup could also make use of displacement sensors or strain gauges to precisely measure the displacement of the chassis. Figure 9 clearly shows an example of such a system. If the displacement could be accurately measured to a precision better than 1/32nd of an inch, experimental error would be largely removed, and the results would be improved.

## Method Comparison

### FEA and Physical Testing Advantages

Finite element analysis offers the ability to make quick, precise, and repeatable models of the chassis which can provide crucial insight into the mechanical properties of the chassis. This allows us to obtain torsional stiffness estimates of multiple chassis design iterations without needing to spend significant amounts of time undergoing full assembly and physical testing. Thus, the major benefit of using FEA models is the significant reduction in overall costs as new iterative models would not need to be tested physically to obtain torsional stiffness estimates. Nor would hand calculations be needed to obtain the deflection response of the chassis. However, there are drawbacks to using FEA, especially if analysis and decision making is informed solely by FEA. Accuracy of the models can vary widely depending on unforeseen geometric factors of the chassis. Furthermore, a finite element analysis result is only as good as the model, which means if the chassis is modeled inadequately or significant portions are oversimplified, it would greatly affect results.

The obvious solution to the limitations of the FEA models is to run more physical tests. Physical testing offers the ability to generate real-world, practical data necessary for informed engineering decisions. It offers far more reliable results that are repeatable due to its vastly increased accuracy. Physical tests are also useful for determining the accuracy of FEA models which can be compared to better understand flaws in the FEA models.

### Comparison Between Methods

Ultimately, considering the ease and cost efficiency of using finite element analysis tools as well as the high accuracy and reliability of the physical test it appears that the best solution is

to use the two methods in tandem with each other to capitalize on their separate yet crucial benefits. This is the long-term plan for this project since, over the course of successive iterations, frequent finite elements models of the chassis will be processed with periodic physical tests. This combination will allow future Senior Design teams the ability to engage in repeated and significant experimentation with chassis design choices that allow them to solve problems much more efficiently, at lower costs and at higher speeds.

# Conclusion

## Summary of Final Results

Throughout this capstone project several key objectives were met. The first objective was to improve the Electric Vehicle Senior Design's performance and structural properties through informed analysis. The results from this goal were highly successful. During the 2022-23 academic year, we were able to use finite element analysis to improve the modeled torsional stiffness of the chassis from 1099 $\frac{N \cdot m}{degree}$ to 1503 $\frac{N \cdot m}{degree}$ by the time the chassis design was released for manufacturing. That corresponds to a torsional stiffness increase of 36.8%. This was done while only increasing the chassis weight by 18.7%. Overall, we minimized the weight of the chassis, the complexity of the chassis, and the number of tubing members in the chassis.

The second goal from this capstone was to create a physical method of testing the chassis to validate the computer models. This goal was also completed as we analyzed, designed, and manufactured a torsional test jig that can model torque applied to the chassis in a way that mirrors the FEA. This testing jig was then used to experimentally gather torsional stiffness values from the physical chassis. A real-world average torsional stiffness value of 1360 $\frac{N \cdot m}{degree}$ was measured which varied only 10% from the expected stiffness value obtained from FEA. This helped to prove the validity of the computer models and provided a framework for future teams to improve on the experimentally gathered data through physical testing.

## Observations and Future Work

The experiments conducted over the course of the semester have been able to demonstrate a sufficient cause and utility for the conduction of torsional stiffness tests on a

Formula SAE chassis for the UAH Senior Design Electric Vehicle project. The finite element models of each iterative step displayed the impact of the information provided by running the torsional stiffness tests on the chassis. Over each iteration explored in this paper, a pattern of a new design revision causing a slight drop in torsional stiffness followed by modifications informed by the finite element analysis leading to an increase in torsional stiffness can be observed. This was done while allowing the new design revisions to retain their functionality as well as manage chassis member count and weight. Throughout the course of the year we optimized complex systems, reduced development time and costs, improved the performance and safety of engineered products, and provided a physical way to test the simulated models. In all, the objectives set to be fulfilled by this capstone at the beginning of the year were accomplished.

While the torsional jig was able to perform the intended tests and provide useful data, there are several facets of its design that can be improved in the future. A more complex system consisting of pivot points, sliders, displacement sensors, and strain gauges can be designed by future teams. This will allow increasingly precise data gathering and comparisons between chassis designs. Subsequent teams are thus tasked with the improvement of physical tests to inform future engineering decisions such as mounting points, placements of additional subsystems, and the full assembly of a driving vehicle.

## References

Chambers, Amy, et al. "Development of a Test Stand for Determining the Torsional Rigidity of a Formula SAE Space Frame." *American Society of Engineering Education*, no. #16580, 26 June 2016. Accessed 8 Mar. 2023.

"FSAE History." *Www.fsaeonline.com*, www.fsaeonline.com/page.aspx?pageid=c4c5195a-60c0-46aa-acbf-2958ef545b72.

Kaneb, Charles. "Tube Frame Analysis." *DesignJudges.com*, Design Judges, 9 Aug. 2022, www.designjudges.com/articles/tube-frame-analysis. Accessed 4 Apr. 2023.

Milliken, Willliam, and Douglas Milliken. "RACE CAR VEHICLE DYNAMICS." *Society of Automotive Engineers*.

Riley, William B., and Albert R. George. Design, Analysis and Testing of a Formula SAE Car Chassis. Tech. no. 2002-01-3300. Warrendale: SAE International, 2002. Print

Tripathi, Satyam, et al. "DESIGN of a FORMULA SAE CHASSIS according to LATERAL LOAD TRANSFER DISTRIBUTION." *International Journal of Research in Engineering and Technology*, vol. 06, no. 07, July 2017, pp. 136–47, https://doi.org/10.15623/ijret.2017.0607023. Accessed 31 Mar. 2023.

Velie, Hubbard D. "Chassis Torsional Rigidity Analysis for a Formula SAE Racecar." MRacing Formula SAE, 2016.